Industrial Engineering Journal
ISSN: 0970-2555
Volume : 55, Issue 03 : 2026

Transient Stability of a Grid-Connected Micro-Hydro Plant: SMIB Modeling and Three-Phase Fault Analysis

Pooja Bansode, Research Scholar, Department of Electrical Engineering
PVPIT, Budhgaon, Sangli, Maharashtra, India
Swapnil Gadgune, Assistant Professor, Department of Electrical Engineering
PVPIT, Budhgaon, Sangli, Maharashtra, India

ABSTRACT
This paper presents the transient stability assessment of a grid-connected run-of-river micro-hydro power plant under a severe symmetrical three-phase-to-ground fault condition. A 100 kVA, 11 kV, 50 Hz synchronous-generator-based micro-hydro system connected to a 220 kV infinite-bus grid through an 11/220 kV step-up transformer is modeled in MATLAB/Simulink. The model integrates a hydraulic turbine-governor, synchronous generator, automatic voltage regulator (AVR), excitation system, transformer, loads, and grid. A three-phase-to-ground fault with Rf = 0.01 Ω is applied from 0.1 s to 0.2 s. System behavior is evaluated through four key variables: terminal voltage Vt, rotor speed ωm, stator current Iabc, and field voltage Vf. Results confirm that Vt recovers after fault clearance, rotor-speed oscillations are damped, stator current returns to normal sinusoidal form, and Vf settles after excitation forcing. The generator maintains synchronism throughout, demonstrating adequate transient stability of the micro-hydro system under the most severe balanced network disturbance.

Keywords: micro-hydro power plant; transient stability; three-phase fault; synchronous generator; MATLAB/Simulink; automatic voltage regulator; hydraulic turbine-governor

1. Introduction

The global transition toward renewable energy has driven rapid integration of distributed generation into modern power grids. Among available renewable options, run-of-river micro-hydro power plants occupy a unique position: unlike solar photovoltaic or wind generation, micro-hydro systems deliver near-continuous energy output wherever adequate water flow exists, providing a reliable and dispatchable source of generation [1]. When such plants are interfaced to the utility grid through synchronous generators, their electromechanical behavior during network disturbances becomes a critical engineering concern that directly affects grid reliability.

Grid-connected micro-hydro plants must fulfill three stability requirements: (a) withstand terminal-voltage disturbances without loss of excitation, (b) contribute rated fault current during short-circuit events to enable protection operation, and (c) preserve rotor synchronism following clearance of those events. Among all network disturbances, the three-phase-to-ground (3Φ-G) fault is the most severe balanced event and constitutes the standard worst-case test for transient stability assessment [2]. During such a fault, generator terminal voltage collapses almost instantaneously, stator current surges to several times rated value, and the resulting mechanical-electrical power mismatch causes rotor acceleration.

Extensive literature covers aspects of micro-hydro plant modeling [3], frequency regulation through governor tuning [4], and terminal voltage control using AVR design [5]. Dynamic modeling of advanced micro-hydro configurations for distributed generation has been reported in [6], and the influence of turbine-governor parameters on grid-connected stability is analyzed in [7]. However, few works simultaneously interpret all four key system variables within a unified time-domain framework that traces the causal chain from fault inception through recovery. This paper addresses that gap by developing a fully parameterized MATLAB/Simulink SMIB model and deriving the complete governing equations from first principles.

Industrial Engineering Journal
ISSN: 0970-2555
Volume : 55, Issue 03 : 2026

II. System Description

The study system is a single-machine infinite-bus (SMIB) configuration. The principal subsystems are: (i) hydraulic turbine-governor, (ii) 100 kVA, 11 kV, 50 Hz synchronous generator, (iii) IEEE Type-1 AVR and excitation system, (iv) 11/220 kV step-up transformer, (v) 50 kW local load on the 11 kV bus, (vi) 100 kW grid-side load on the 220 kV bus, and (vii) a 10,000 MVA infinite-bus grid. A three-phase-to-ground fault block (Rf = 0.01 Ω) is placed on the 220 kV bus to simulate the disturbance. The pictorial system schematic is shown in Fig. 1.

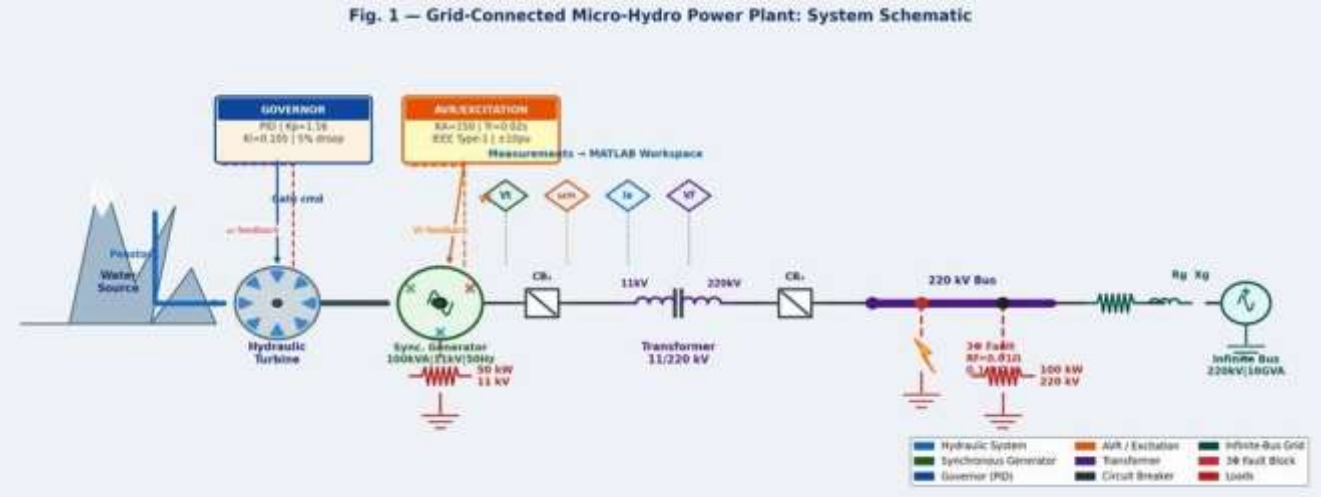

Fig. 1 — Grid-Connected Micro-Hydro Power Plant: Pictorial System Schematic

III. Mathematical Modeling

This section derives the governing equations of every subsystem from first principles. All quantities are in per-unit (pu) unless otherwise stated.

A. Per-Unit System Bases

The following base quantities are chosen for normalisation on the generator LV side:

$$S_{base} = 100\,kVA,\ V_{base,LV} = 11\,kV,\ V_{base,HV} = 220\,kV \quad (1)$$

From these, base current and base impedance on each voltage level are derived as:

$$I_{base} = \frac{S_{base}}{\sqrt{3} \times V_{base}},\ Z_{base} = \frac{V_{base}^{\ 2}}{S_{base}} \quad (2)$$

$$\omega_b = 2\pi f = 2\pi \times 50 = 314.16\,rad/s \quad (3)$$

B. Synchronous Generator — dq-Axis Equations

The synchronous generator is modeled in the Park (dq0) rotating reference frame aligned with the rotor field axis. This transformation decouples the three-phase stator quantities into time-invariant DC values at steady state.

1) Flux-Linkage Equations

The d-axis and q-axis stator flux linkages are:

$$\psi_d = -X_d \cdot i_d + X_{md} \cdot i'_{fd} \quad (4)$$

$$\psi_q = -X_q \cdot i_q \quad (5)$$

2) Stator Voltage Equations

Applying Kirchhoff's voltage law in the dq frame, including resistive drop, transformer EMF (dψ/dt), and rotational EMF (ωmψ terms):

$$v_d = -R_s \cdot i_d + \frac{d\psi_d}{dt} - \omega_m \cdot \psi_q \quad (6)$$

$$v_q = -R_s \cdot i_q + \frac{d\psi_q}{dt} + \omega_m \cdot \psi_d \quad (7)$$

3) Electromagnetic Power and Terminal Voltage

$$P_e = v_d \cdot i_d + v_q \cdot i_q \quad (8)$$

$$V_t = \sqrt{v_d^2 + v_q^2} \quad (9)$$

4) Field Winding Dynamics

$$T'_{do} \cdot \frac{dE'q}{dt} = E_{fd} - E'q - (X_d - X'd) \cdot i_d \quad (10)$$

C. Rotor Dynamics — Swing Equation

Applying Newton's second law to the rotor mass, the electromechanical swing equation in per-unit form is:

$$\frac{2H}{\omega_s} \cdot \frac{d\omega_m}{dt} = P_m - P_e - D \cdot (\omega_m - 1) \quad (11)$$

where H = 3.2 s is the machine inertia constant, ω_s = 1.0 pu is the synchronous speed reference, P_m is mechanical power, P_e is electrical air-gap power, and D is the damping coefficient.

Accelerating power and rotor angle dynamics are:

$$P_{acc} = P_m - P_e \quad (12)$$

$$\frac{d\delta}{dt} = \omega_b \times (\omega_m - 1) \quad (13)$$

The transient stability criterion requires that δ(t) remains bounded and returns to a stable equilibrium after fault clearance:

$$|\delta(t)| < \delta_{max} \implies Stable\ (synchronism\ maintained) \quad (14)$$

D. Hydraulic Turbine-Governor Model

The governor senses rotor-speed deviation and adjusts turbine gate opening to restore balance. The speed error is:

$$e_\omega(t) = \omega_{ref} - \omega_m(t) = 1.0 - \omega_m(t) \quad (15)$$

A PID controller processes this error to produce the gate control signal:

$$u_g(t) = K_p \cdot e_\omega(t) + K_i \int e_\omega(t)\, dt + K_d \cdot \frac{de_\omega}{dt} \quad (16)$$

The gate servomotor is modelled as a first-order lag:

$$T_a \cdot \frac{dg}{dt} + g = K_a \cdot u_g(t) \quad (17)$$

Mechanical power from the hydraulic turbine is governed by the water-hammer equation:

$$T_w \cdot \frac{dP_m}{dt} + P_m = g(t) \quad (18)$$

where T_w = 2.67 s is the water starting time. Governor droop is set to 5%:

$$R_{droop} = \frac{\Delta\omega}{\Delta P_g} = 0.05\ pu/pu \quad (19)$$

E. Automatic Voltage Regulator and Excitation System

The IEEE Type-1 AVR regulates terminal voltage by controlling field voltage V_f. The voltage error signal is:

$$e_v(t) = V_{ref} - V_t(t) = 1.0 - V_t(t) \quad (20)$$

The first-order AVR regulator transfer function in time-domain form is:

$$T_r \cdot \frac{dV_f}{dt} + V_f = K_A \cdot e_v(t) \quad (21)$$

Field voltage is physically limited by the exciter ceiling:

$$V_{f,min} \le V_f \le V_{f,max} \implies -10\,pu \le V_f \le +10\,pu \quad (22)$$

F. Network Model and Fault Representation

The 11/220 kV transformer is represented by its leakage impedance: $R_T = 0.01$ pu, $X_T = 0.05$ pu. The infinite bus provides a constant-voltage, constant-frequency reference: $V_\infty = 1.0\angle 0°$ pu at 220 kV, 50 Hz, with $S_{sc} = 10{,}000$ MVA and X/R = 10.

The symmetrical three-phase-to-ground fault is modelled as a shunt impedance $Z_f = R_f + j0$ suddenly appearing at the 220 kV bus. The fault current magnitude is:

$$I_f = \frac{V_{prefault}}{Z_{th} + Z_f} \quad (23)$$

For the sub transient first-peak fault current at the generator terminals:

$$I_{f,peak} \approx \frac{E''q}{X''d + X_T + Z_f} \quad (24)$$

Table I summarises all key generator, network, and control parameters.

Table I. Model Parameters Summary

Parameter	Symbol	Value	Unit
Rated apparent power	S_n	100	kVA
Rated terminal voltage (LV)	V_n,LV	11	kV
Rated frequency	F	50	Hz
Stator resistance	R_s	0.00285	pu
d-axis sync. reactance	X_n	1.305	pu
d-axis transient reactance	X'_n	0.296	pu
d-axis subtransient reactance	X''_n	0.252	pu
q-axis reactance	X_v	0.474	pu
Inertia constant	H	3.2	s
d-axis transient OC time constant	T'_{no}	5.044	s
d-axis subtransient OC time constant	T''_{no}	0.053	s
Water starting time	T_u	2.67	s
Governor servo time constant	T_a	0.07	s
Governor PID gains	Kp / Ki / Kd	1.16/0.105/0	pu

Industrial Engineering Journal
ISSN: 0970-2555
Volume : 55, Issue 03 : 2026

Speed droop	R_n	5	%
AVR gain	K_a	150	pu/pu
AVR time constant	T_r	0.02	s
Field voltage limits	V_e,min/max	−10/+10	pu
Transformer impedance	RT / XT	0.01/0.05	pu
Grid short-circuit level	S_s^c	10,000	MVA
Fault resistance	R_e	0.01	Ω
Fault duration	Δt_e	100	ms

IV. Simulation Setup

The mathematical model from Section III is implemented in MATLAB/Simulink as a fully integrated SMIB system. Fig. 2 shows the complete simulation block and circuit diagram using standard engineering symbols. Each subsystem — turbine-governor, synchronous generator (dq model), AVR-excitation, transformer, circuit breakers, fault block, loads, and infinite-bus grid — is a dedicated Simulink subsystem connected through appropriate signal interfaces.

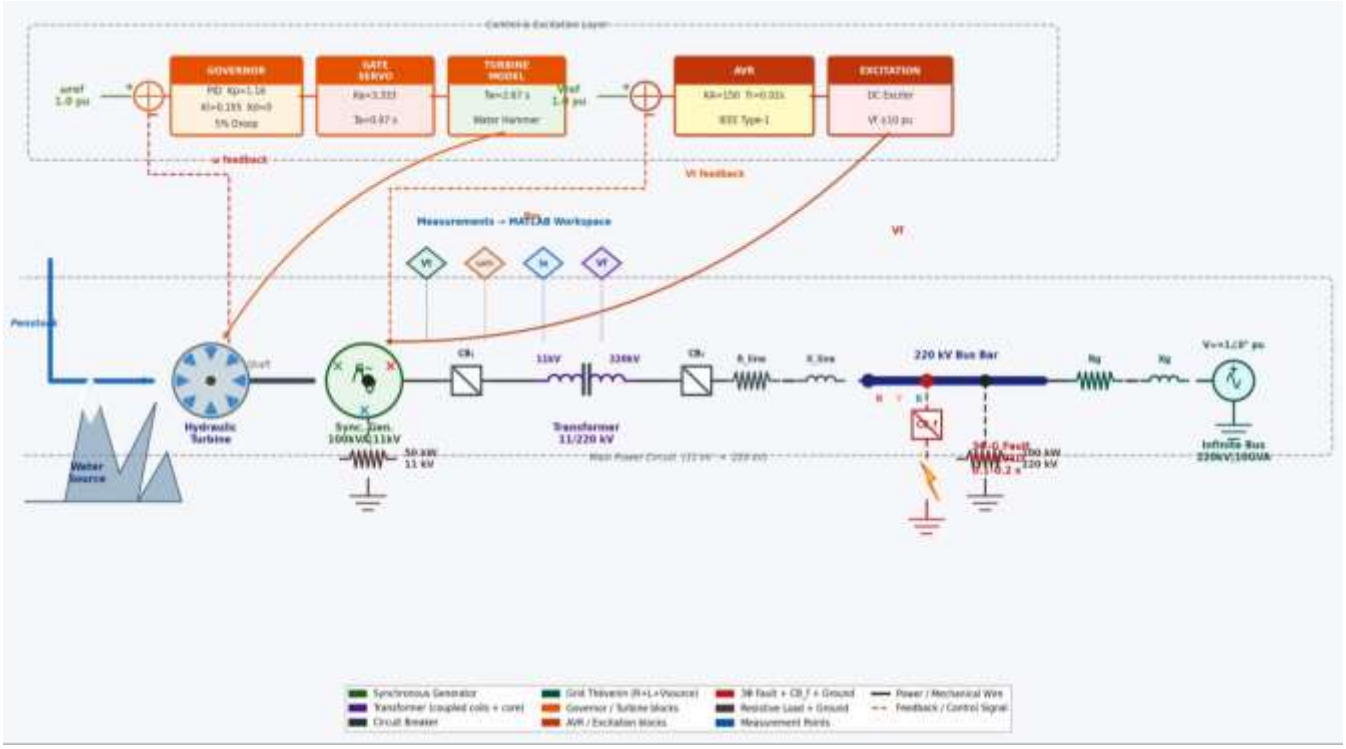

Fig. 2 — Transient Stability Assessment: System Block & Circuit Diagram with Standard Engineering Symbols

The simulation is initialized to the pre-fault steady-state operating point: $V_t = 1.0$ pu, $\omega_m = 1.0$ pu, $P_m = P_e = 0.8$ pu. The ODE solver ode23tb (stiff/TR-BDF2) is used with a maximum step of 50 μs.

Three simulation intervals are defined:

Industrial Engineering Journal
ISSN: 0970-2555
Volume : 55, Issue 03 : 2026

- Pre-fault (0–0.1 s): steady-state baseline
- Fault active (0.1–0.2 s): 3Φ-G fault with $R_f = 0.01\ \Omega$ applied
- Post-fault recovery (0.2 s onward): fault cleared, free-response damping

V. Results and Discussion

Fig. 3 presents the time-domain simulation results for all four state variables. The fault zone (0.1–0.2 s) is highlighted in red on each subplot.

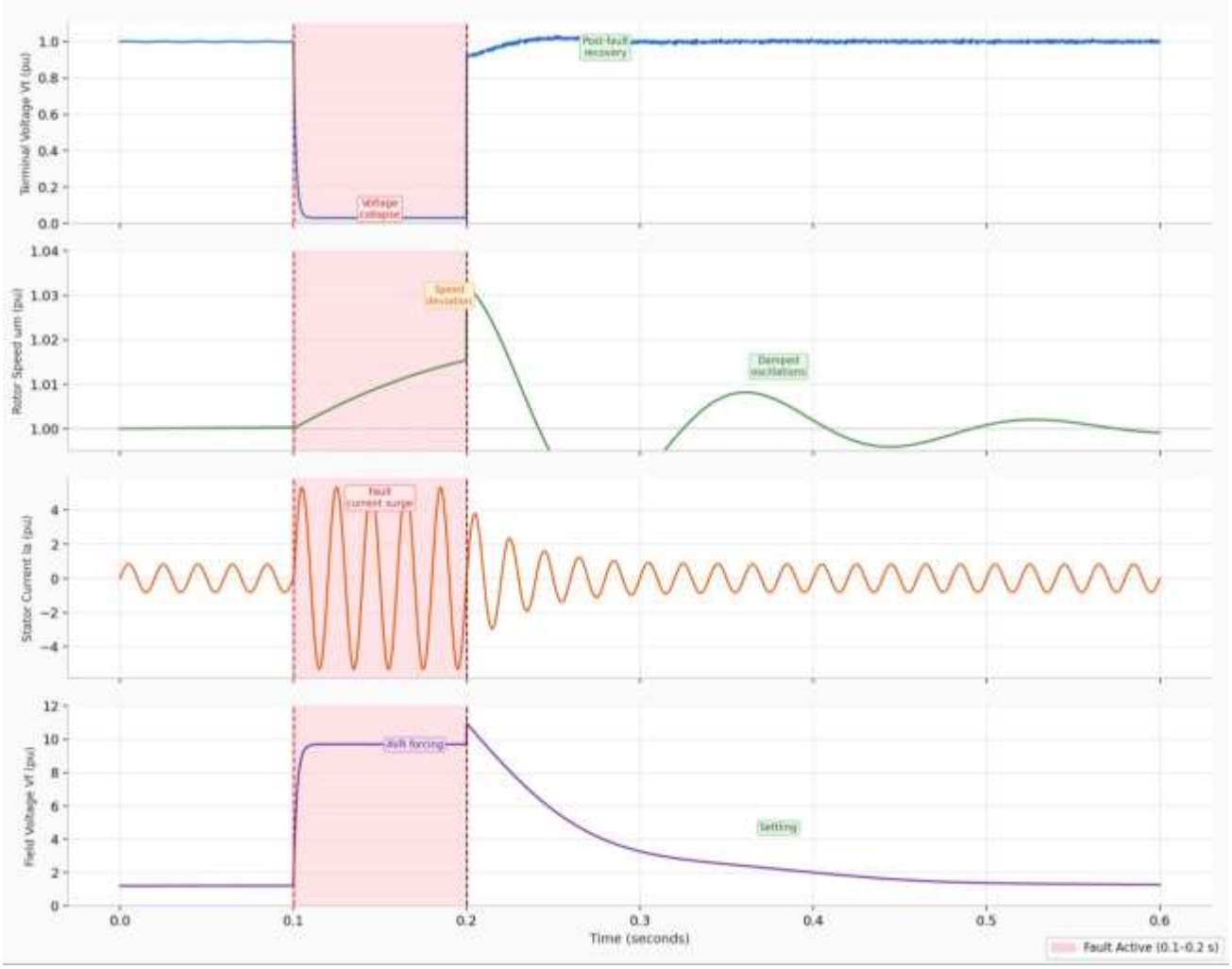

Fig. 3 — Simulated Transient Stability Results: (a) Terminal Voltage V_t, (b) Rotor Speed ω_m, (c) Stator Current $I_{aB}{}^c$, (d) Field Voltage V_e | Fault: 0.1–0.2 s, Rf = 0.01 Ω

A. *Terminal Voltage V_t*

Pre-fault: $V_t \approx 1.0$ pu, confirming stable steady-state AVR regulation. Fault inception (t = 0.1 s): the 3Φ-G fault places $Z_f = 0.01\ \Omega$ across the 220 kV bus, driving $V_t \rightarrow 0$ as shown by equation (9). Fault clearance (t = 0.2 s): V_t begins recovering immediately, driven by AVR excitation forcing (equation 21) and network voltage restoration. The voltage trace returns toward 1.0 pu without sustained depression, confirming voltage stability.

B. *Rotor Speed ω_m*

Pre-fault: $\omega_m = 1.0$ pu (50 Hz). Fault period: when $P_e \rightarrow 0$, the hydraulic turbine constrained by $T_w = 2.67$ s continues supplying $P_m \approx 0.8$ pu. The accelerating power $P_{acc} = P_m - P_e \approx 0.8$ pu drives ω_m above 1.0 pu per equation (11). Post-fault: the governor detects speed error (equation 15) and closes

the gate per equation (16)–(18). Rotor-speed oscillations are visibly damped, converging to 1.0 pu, satisfying stability criterion (14).

C. Stator Current I_{abc}

Pre-fault stator current is balanced three-phase sinusoidal at ≈0.82 pu. At fault inception, current surges to the subtransient level defined by equation (24). After t = 0.2 s, current returns to approximately sinusoidal waveform, confirming successful fault removal without sustained overcurrent.

D. Field Voltage V_e

Pre-fault: V_f is at its steady-state setpoint with small voltage error. Fault period: terminal voltage collapse drives $e_v(t) \rightarrow 1.0$ pu, forcing V_f toward the +10 pu ceiling per equation (21)–(22). Post-fault: as V_t recovers, e_v diminishes and V_f decays smoothly with time constant $T_r = 0.02$ s. The monotonic settling confirms excitation-system stability without AVR windup.

E. Integrated Causal Analysis and Stability Assessment

The four responses are causally linked:

① Fault at t = 0.1 s → $Z_f \approx 0$ on 220 kV bus
② $V_t \rightarrow 0$ (eq. 9) → $P_e \rightarrow 0$ (eq. 8)
③ $P_{acc} = P_m - P_e \approx 0.8$ pu → $\omega_m \uparrow$ (eq. 11–12)
④ $e_v \rightarrow 1.0$ pu → AVR forces $V_f \rightarrow +10$ pu (eq. 20–22)
⑤ Fault cleared t = 0.2 s → Z_f removed
⑥ V_t recovers → P_e restores → $P_{acc} < 0 \rightarrow \omega_m$ decelerates
⑦ Governor closes gate via eq. (16)–(18) → oscillations damp → $\omega_m \rightarrow 1.0$ pu
⑧ V_f settles → V_t stabilises at 1.0 pu; eq. (14) satisfied → Stable

Table II. Transient Performance Indices

Performance Index	Observed Result	Interpretation
Min. terminal voltage Vt (fault period)	Near-zero pu	Severe voltage dip
Vt recovery onset after clearance	Immediately (t > 0.2 s)	AVR pre-charges excitation
Max. rotor-speed deviation Δωmax	Temporary rise > 1.0 pu	Bounded acceleration
Rotor-speed oscillation character	Damped → 1.0 pu	Synchronism retained
Peak stator current Iabc,max	Several × rated (eq. 24)	Subtransient fault current
Peak field voltage Vf,max	≈10 pu (AVR ceiling)	Max. excitation forcing
Field voltage post-fault settling	Smooth decay to SS	AVR stable, no windup
Overall synchronism status	MAINTAINED — STABLE	Transient stability confirmed

VI. Conclusion

This paper presented a comprehensive transient stability study of a 100 kVA grid-connected micro-hydro power plant under a severe 100 ms three-phase-to-ground fault, implemented in MATLAB/Simulink. The mathematical model was derived from first principles — encompassing Park's dq-axis generator equations (4)–(10), the electromechanical swing equation (11)–(14), hydraulic turbine-governor dynamics (15)–(19), and IEEE Type-1 AVR equations (20)–(22) — and validated through time-domain simulation.

The four key findings are:

① Terminal voltage V_t collapses to near zero during the fault but recovers to nominal immediately after clearance, sustained by AVR excitation forcing (eq. 21).

② Rotor-speed deviation is temporary and bounded; post-fault oscillations are visibly damped (eq. 11), confirming stability criterion $|\omega_m(t) - 1| \rightarrow 0$ is satisfied.

③ Stator current surges to the subtransient fault level (eq. 24) during the fault and returns to rated sinusoidal form after fault removal.
④ Field voltage is forced to the AVR ceiling (+10 pu) during the fault and settles smoothly to steady state, confirming coordinated excitation-system operation.

The coordinated action of the hydraulic turbine-governor and the AVR is essential for stable recovery. The developed framework is directly extensible to: optimised PID / fuzzy-logic / model-predictive governor design; asymmetrical fault analysis; islanded-operation studies; and hardware-in-the-loop validation — forming the immediate future scope of this work.

References

[1] T. Adefarati and R. C. Bansal, "Integration of renewable distributed generators into the distribution system: A review," IET Renewable Power Generation, vol. 10, no. 7, pp. 873–884, 2016.
[2] P. Kundur, Power System Stability and Control. New York, NY, USA: McGraw-Hill, 1994.
[3] A. E. Hamdaouy, I. Salhi, S. Doubabi, N. Essounbouli, and M. Chennani, "An integrated approach for modeling three-phase micro hydropower plants," European Journal of Electrical Engineering, vol. 21, no. 6, pp. 479–486, 2019.
[4] I. Salhi, S. Doubabi, N. Essounbouli, and A. Hamzaoui, "Frequency regulation for large load variations on micro-hydro power plants with real-time implementation," International Journal of Electrical Power & Energy Systems, vol. 60, pp. 6–13, 2014.
[5] N. Sanampudi and P. Kanakasabapathy, "Integrated voltage control and frequency regulation for stand-alone micro-hydro power plant," Materials Today: Proceedings, vol. 46, pp. 5027–5031, 2021.
[6] J. Márquez, M. G. Molina, and J. M. Pacas, "Dynamic modeling, simulation and control design of an advanced micro-hydro power plant for distributed generation applications," International Journal of Hydrogen Energy, vol. 35, no. 11, pp. 5772–5777, 2010.
[7] G. Zangmo, K. Om, and K. Uhlen, "Impact of hydro-turbine and governor parameters on stability of grid connected power system," International Journal on Electrical Engineering and Informatics, vol. 9, no. 2, pp. 222–234, 2017.